Quantitative analysis of trace element concentrations in some gem-quality diamonds

2009 J. Phys.: Condens. Matter 21 364207

(http://iopscience.iop.org/0953-8984/21/36/364207)

J. Phys.: Condens. Matter **21** (2009) 364207 (13pp) doi:10.1088/0953-8984/21/36/364207

Quantitative analysis of trace element concentrations in some gem-quality diamonds

J McNeill[1], D G Pearson[1], O Klein-BenDavid[1,2], G M Nowell[1], C J Ottley[1] and I Chinn[3]

[1] Northern Centre for Isotopic and Elemental Tracing, Department of Earth Sciences, Durham University, South Road, Durham DH1 3LE, UK
[2] Institute of Earth Sciences, The Hebrew University, Jerusalem, 91904, Israel
[3] De Beers Group Exploration, Johannesburg, South Africa

Received 5 April 2009, in final form 8 May 2009
Published 19 August 2009
Online at stacks.iop.org/JPhysCM/21/364207

Abstract

The geochemical signature of diamond-forming fluids can be used to unravel diamond-forming processes and is of potential use in the detection of so-called 'conflict' diamonds. While fluid-rich fibrous diamonds can be analyzed by a variety of techniques, very few data have been published for fluid-poor, gem-quality diamonds because of their very low impurity levels. Here we present a new ICPMS-based (ICPMS: inductively coupled plasma mass spectrometry) method for the analysis of trace element concentrations within fluid-poor, gem-quality diamonds. The method employs a closed-system laser ablation cell. Diamonds are ablated and the products trapped for later pre-concentration into solutions that are analyzed by sector-field ICPMS. We show that our limits of quantification for a wide range of elements are at the sub-pg to low pg level. The method is applied to a suite of 10 diamonds from the Cullinan Mine (previously known as Premier), South Africa, along with other diamonds from Siberia (Mir and Udachnaya) and Venezuela. The concentrations of a wide range of elements for all the samples (expressed by weight in the solid) are very low, with rare earth elements along with Y, Nb, Cs ranging from 0.01 to 2 ppb. Large ion lithophile elements (LILE) such as Rb and Ba vary from 1 to 30 ppb. Ti ranges from ppb levels up to 2 ppm.

From the combined, currently small data set we observe two kinds of diamond-forming fluids within gem diamonds. One group has enrichments in LILE over Nb, whereas a second group has normalized LILE abundances more similar to those of Nb. These two groups bear some similarity to different groups of fluid-rich diamonds, providing some supporting evidence of a link between the parental fluids for both fluid-inclusion-rich and gem diamonds.

(Some figures in this article are in colour only in the electronic version)

1. Introduction

Perhaps the most important information required to understand the origin of diamonds is the nature of the fluid that they crystallize from. Progress in constraining the identity of the diamond-forming fluid for high-purity gem diamonds that contain very low concentrations of fluid inclusions has been hampered by analytical challenges. In contrast, significant recent advances have been made in the understanding of fluids that are parental to fibrous diamonds. Such diamonds are fluid-rich and hence amenable to analysis via a number of different methods. It is an assumption throughout this paper that even 'ultra-pure' gem diamonds will contain small amounts of sub-microscopic fluid or melt inclusions and that any net ablated diamond material will contain the contents of these inclusions as well as other lattice impurities and substitutions. Early studies of the major element composition of fibrous, fluid-rich diamonds recognized the K-rich nature of the entrapped fluids and suggested a link to kimberlitic magmatism (Navon *et al* 1988). Subsequent studies of the trace element systematics of these fluid-inclusion-rich diamonds using either INAA (Schrauder *et al* 1996) or LA–ICPMS (Resano *et al* 2003,

Tomlinson *et al* 2005, 2006, 2009, Rege *et al* 2005, Zedgenizov *et al* 2007, Weiss *et al* 2008a, 2008b) have supported this early conclusion, with some studies invoking carbonatite instead of kimberlite as a parental fluid. While the trace element evidence appears convincing, and was supported by sparse Sr isotope data (Akagi and Matsuda 1998), more recent Sr and Nd isotope measurements on a wide variety of fluid-rich diamonds have pointed to additional components, some derived from ancient enriched mantle lithosphere (Klein-BenDavid *et al* 2008).

While there has been a surge in compositional data constraining the origin of fluid-rich diamonds, available data for fluid-poor gem-quality diamonds remain very sparse, largely because of the exceedingly low levels of elemental impurities that they contain. Since the early studies of Fesq *et al* (1975) and Bibby (1982) few data have been published and no elemental data have appeared that are demonstrably quantitative in nature. In this study we describe a new ultra-low-level method for the quantitative analysis of fluid-poor gem diamonds and present data from a suite of diamonds from the Cullinan Mine, South Africa plus additional samples from Udachnaya, Siberia. We demonstrate the quantitative nature of the data and discuss the limitations of applying only 'limits of detection' as a criterion for screening data. We compare trace element signatures for diamonds of both 'eclogitic' and 'peridotitic' parageneses and evaluate the trace element systematics of these diamonds with respect to those from fluid-inclusion-rich, non-gem diamonds.

2. Samples and standards

2.1. Diamonds

We have measured the trace element concentrations in diamonds from three regions. The majority of samples come from the Cullinan Mine (formerly Premier Mine), South Africa and have been previously characterized by cathodoluminescence (CL) and Fourier transform infra-red spectroscopy (FTIR) by Chinn *et al* (2003). In addition, two samples have been analyzed from Siberia, one from Udachnaya (3812) and one from Mir (1581). A single diamond from Venezuela (PHN5921) has also been analyzed.

The 10 Cullinan diamonds analyzed for trace elements (figure 1) are a sub-set of 20 polished plates. These plates ranged between 0.2 and 0.5 carats. Samples were selected for trace element study on the basis of their silicate inclusion paragenesis so that diamond trace element systematics can be compared with paragenesis to examine potential differences and similarities between diamond-forming fluids in the two petrologically distinct paragenetic environments. Two of the Cullinan diamonds were identified as belonging to the peridotitic (P-type) paragenesis (AP28 and AP30) and eight were identified as belonging to the eclogitic (E-type) paragenesis (Chinn *et al* 2003). One of the P-type stones (AP28) contained a chrome-diopside inclusion and was identified by FTIR as a Type II (nitrogen free) diamond. All samples analyzed for trace elements are colorless and while they contain solid inclusions, there are no obvious zones containing fluid inclusions of the type seen in fibrous or cloudy diamonds (e.g., Navon *et al* 1988, Izraeli *et al* 2004).

The Udachnaya, Mir and Venezuelan samples were 0.6, 0.5 and 0.1 carats respectively. Sample 3812, a plate cut from an octahedron from Udachnaya, is of P-type paragenesis, as is common with Udachnaya inclusion-bearing diamonds, and hosts a sulfide inclusion with 15 wt% Ni. Sample 1581, from Mir, is also a plate, cut from an octahedron, is of E-type paragenesis, containing a low-Ni (5.2 wt%) sulfide inclusion. PHN5921 is of P-type paragenesis and contained a lherzolitic garnet inclusion.

3. Geology of diamond sample sources

3.1. Cullinan, South Africa

The Cullinan kimberlite is located 30 km ENE of Pretoria in the Central Terrain of the Archean Kaapvaal Craton (de Wit *et al* 1992) and is of Meso-Proterozoic age (∼1180 Ma; Richardson *et al* 1993). Multiple phases of kimberlite intrusion and subsequent alteration exist. All of these phases are diamond bearing (Deines *et al* 1984). The kimberlite is cut by a 1100 Ma gabbroic sill and penetrates a norite phase of the Bushveld Complex. Cullinan Mine is renowned for the recovery of large, high value Type II (nitrogen free) diamonds such as the Cullinan.

3.2. Udachnaya, Siberia

The diamondiferous Udachnaya kimberlite pipe is located in the Daldyn-Alakit region of the Siberian kimberlite province. At the surface the pipe consists of two adjacent bodies which differ considerably in terms of mineralogy, petrology, composition and degree of alteration. Radiometric dating indicates intrusion at 367 ± 4 Ma (Kinny *et al* 1997, Pearson *et al* 1997, Maas *et al* 2005). The diamond population from the Udachnaya pipes has a high proportion of cuboid diamonds containing abundant fluid microinclusions. Most microinclusions in cuboid stones from Udachnaya have been classed as 'carbonatitic' in character (carbonate-rich compositions with (water/(water + carbonate)∼0.05–0.2) and fall in the lower end of the hydrous-silicic to carbonatitic join observed in Botswanian diamonds (Navon *et al* 1988, Schrauder and Navon 1994). Within the gem-diamond population most Udachnaya stones containing silicate or sulfide inclusions belong to the peridotitic paragenesis (Bulanova 1995, Pearson *et al* 1999). Additional information on Udachnaya diamonds has been summarized by Bulanova (1995) and Spetsius and Taylor (2008).

3.3. Mir, Siberia

The Mir kimberlite is thought to be 350 Ma in age and is located in the southern part of the Siberian platform Kimberlite field. The gem-diamond population from Mir that contain silicate or sulfide inclusions are dominated by those of eclogitic paragenesis (Bulanova 1995).

3.4. Venezuela

The Venezuelan diamond originated from the Guaniamo alluvial diamond field and hence its parent volcanic intrusion

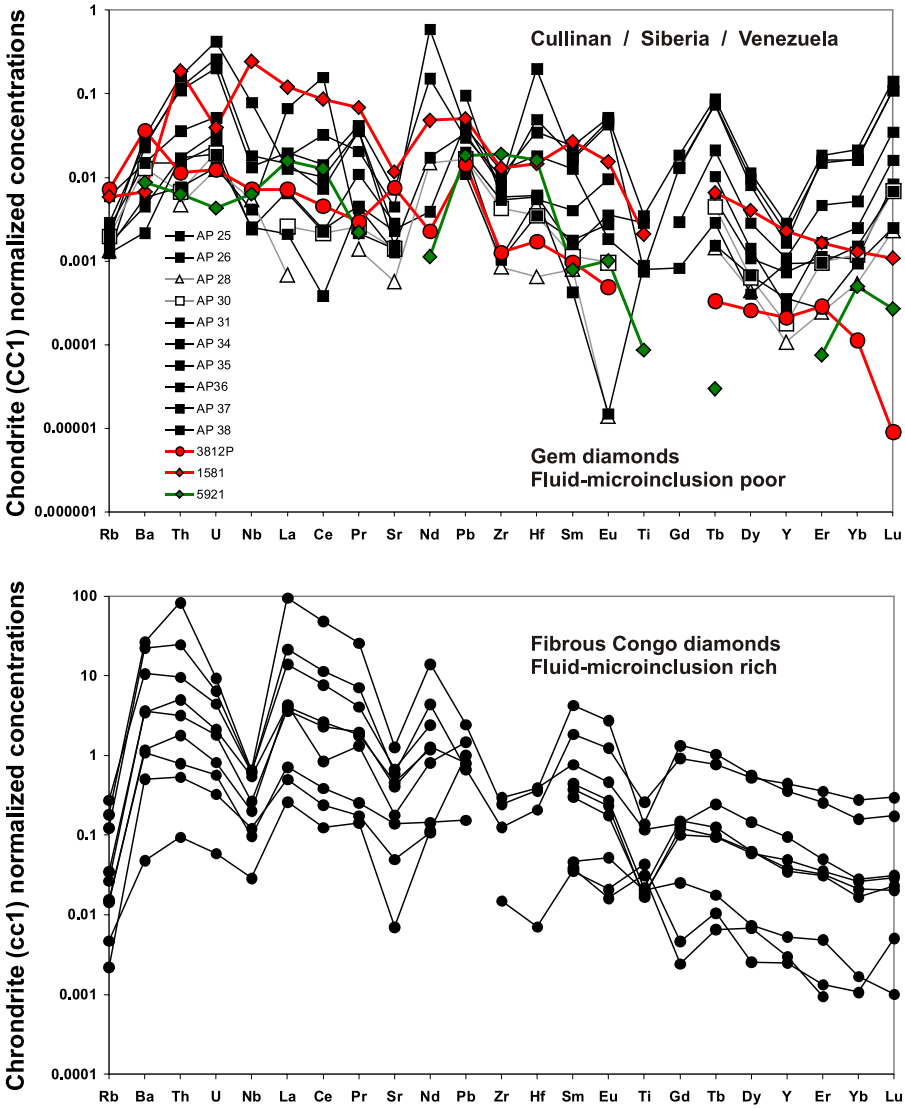

Figure 1. Top: chondrite-normalized trace elemental concentrations in the Cullinan diamonds, the two Siberian diamonds, and the one Venezuelan sample analyzed in this study. Bottom: trace element concentration from a suite of fibrous, fluid-microinclusion-rich diamonds that display similar inter-element fractionation patterns to the gem diamonds from Cullinan and Siberia.

is unknown. A major element analysis of the Cr-pyrope garnet inclusion from this diamond is provided in Nixon *et al* (1994) along with other details of diamonds recovered from the Guaniamo field.

4. Analytical methods

4.1. CL

Prior to this study cathodoluminescence images on all Cullinan diamond plates were acquired by Chinn *et al* (2003) using a Technosyn cold cathode CL attachment, operating at 810 μA and 12 kV. Diamonds 3821 and 1581 have also been studied by CL. No CL images are available for PHN5921.

4.2. FTIR

Spectra were acquired by Chinn *et al* (2003) with a Nicolet Magna 760-IR spectrometer, over the infra-red range from 4000 to 650 cm^{-1}. An aperture of 100 μm was used at a resolution of 8 cm^{-1}. Deconvolution of baselined spectra was performed using a least squares fit of the A, B and D components. Absorption coefficients of 16.5 and 79.4 ppm cm^{-1} for the A and B components respectively were used (Boyd *et al* 1994, 1995).

4.3. Trace element analysis—a new approach

4.3.1. Experimental. All laboratory and analytical work for this study was carried out in the Arthur Holmes Isotope Geology Laboratory at the Department of Earth Science, University of Durham. All low concentration work was conducted in custom-built class 100 laminar flow environments. Dedicated reagent bottles and teflon beakers were used to obtain consistent ultra-low-level chemistry. Ultra-pure water with a resistivity of ∼18.2 MΩ was obtained from a Milli-Q Element system. Reagents used for sample recovery

and dilution for mass spectrometry were ultra-purity triple-distilled acids (UpA) manufactured by Romil Ltd. Working solutions of reagents are made up from these stock acids by diluting with Milli-Q purity water.

4.3.2. Ablation

4.3.2.1. Off-line ablation cell. While we use both laser ablation and ICPMS for multi-element trace analysis of diamonds we differ from previous approaches (Resano *et al* 2003, Tomlinson *et al* 2005, 2006, 2009, Rege *et al* 2005) in that we utilize an 'off-line', closed-system ablation cell that is not connected to the mass spectrometer. This allows us to control analyte levels by varying the duration of ablations. The resulting signals for most analytes are considerably elevated above instrumental background compared with direct ablation techniques, permitting more precise accurate quantitative measurement.

For this study we employed a New Wave™ Nd:YAG 213 nm laser to ablate all diamonds. The standard New Wave™ open-system ablation cell is replaced with a custom-manufactured cell of our own design that consists of a PTFE body that can be acid cleaned between ablations, and a screw-on laser window. Since our off-line ablation cell is a sealed unit, material is retained within the cell during the ablation such that laser-induced elemental fractionation at the ablation site, which is a major problem for on-line laser ablation analysis, poses no problem. This system was originally developed for the analysis of Sr–Nd–Pb isotopic ratios in fluid-rich fibrous diamonds (Klein-BenDavid *et al* 2008) and has been adapted for trace element determinations.

The internal volume of our off-line ablation cell is approximately 5 ml. It comprises three components—a main vessel that houses the sample, a removable laser window/PTFE cap and a screw cap, which retains the laser window. The laser window is UV grade fused silica and is coated on the upper surface, which faces the incident laser beam, with an anti-reflection coating transparent to wavelengths of 193–248 nm.

The main vessel has an outer diameter of ∼30 mm and a similar depth. An internal plinth with a slight central recess allows controlled placement of the sample in the center of the cell. The PTFE construction of the cell allows it to be acid cleaned between analyses. Prior to each ablation the cell is leached in 6N HCl (2 × 24 h) at 120 °C to remove any memory of a previous sample. The main compartment and parts are then immersed in 2N HNO_3 for 24 h at 80 °C followed by a Milli-Q H_2O bath (2 × 24 h). The last stage involved a further 120 °C leach in UpA 6N HCl (2 × 24 h).

4.3.2.2. Sample preparation and ablation. Prior to ablation diamond samples are washed in an ultra-sonic bath for 120 min in a 1:1 16N HNO_3:29N HF solution before being rinsed in MQ H_2O and leached in 6N HCl for 24 h. The diamonds are then dried at 100 °C for 60 min, weighed on a Mettler Toledo™ UMT2 Micro Balance with an uncertainty of ±0.1 μg (1 std deviation; determined on 200 replicates).

The diamond to be analyzed is mounted within the ablation cell, held under its own weight, or fused into a perfluoroalkoxy (PFA) Teflon disk, atop a raised circular plinth. Care is taken to ensure a flat surface is presented to the laser. Once the diamond is in place the ablation cell is capped with the laser window. The windows are pre-leached for 24 h in dilute HNO_3 and rinsed and stored in MQ H_2O. Immediately prior to replacing the ablation cell lid the laser window is dried in a high-purity argon gas-steam. The laser window is blank tested in every diamond analysis and consistently contains no contaminants.

4.3.2.3. Laser parameters. During ablation we operate the New Wave™ laser with a frequency of 20 Hz at 100% output, producing an ablation energy of ∼1 mJ on the sample and a fluence (energy density) of 5–6 J cm^{-2} based on a beam diameter of 160 μm (table 1). The duration of the ablation is varied depending on the expected analyte levels within the diamond and the signal intensity that we are aiming for. These factors also control the size of the resulting ablation pits. For the analysis of gem diamonds with extremely low trace element concentrations we employ a raster pattern that avoids any visible solid inclusions. Typical ablation pits on the diamond surface have X–Y dimensions of 50–250 μm and a depth of 10–50 μm. For the analysis of the Cullinan diamonds presented here, which are large plates with very low suspected trace element abundances, larger raster patterns (X–Y: 500 μm × 500 μm) were used requiring ablation times of 180 min. While this extended ablation time is considerably longer than those used in recently published 'direct ablation' studies (i.e. normal LA-ICMPS techniques; Rege *et al* 2005, Zedgenizov *et al* 2007, Weiss *et al* 2008a, 2008b), which are typically 130 s, the gain is in the much larger measured analyte signals during mass spectrometry, with resulting gains in limits of quantification (see below).

4.3.2.4. Post-ablation procedure. Following ablation the cell was opened in a Class 100 HEPA-filtered environment. 3 ml of 6N HCl was added to the ablation cell, covering the diamond and plinth. The cell was re-sealed with a pre-cleaned PTFE lid (which replaces the laser window), shaken vigorously for 60 s and then placed in an ultra-sonic bath filled with reverse osmosis water for 35 min. The laser window was dealt with separately. It is placed sample-side down on a custom-made PTFE crux attached to a pre-cleaned 7 ml PFA screw-cap vial containing 1 ml UpA 6N HCl. After leaching in this solution at 80 °C for 35 min the sample side of the window was rinsed with Milli-Q H_2O into the same vial. The ablation cell solution was then transferred to the 7 ml PFA vial containing the laser-window deposit. Care was taken to agitate the diamond ablation pit surface followed by refluxing with the acid to ensure maximum material recovery. Tuning laser parameters for application to each specific sample avoids the possibility of their being any solid residue left behind in the ablation cell after acid collection. The diamond material is completely vaporized. The combined solution was dried down at 120 °C and the residue then taken up in 250 μl 3% UpA HNO_3 and allowed to digest fully for 48 h at 120 °C before being transferred to pre-leached 1.5 ml micro-tubes. This solution was then ready for ICPMS analysis. The ablated diamond was rinsed multiple

Table 1. Instrumental parameters typical during a full-method analysis of diamond samples.

LA New Wave Nd:YAG		ICPMS Thermo ELEMENT2	
Laser source	New Wave	Nebulizer	25 μl min^{-1} micromist Teflon PFA concentric nebulizer
Wavelength	213 nm		
		Spray chamber	ESI stable introduction system quartz dual spray chamber
Power			
Energy	0.0–1.1 mJ		
Energy density	5–6 J cm^{-2}	RF power	1300 W
Output	100%	Plasma gas flow	16 l min^{-1}
Rep. rate	20 Hz	Auxiliary gas flow	1 l min^{-1}
		Nebulizer gas flow	$\sim$0.95 l min^{-1}
Spot size	160 μm	Resolution	300 (low)
Scan speed	50 μm s^{-1}		
Depth/pass	2 μm	Isotopes measured	Ti49, Rb85, Sr88, Y89, Zr90, Nb93, Cs133, Ba137, La139, Ce140, Pr141, Nd143, Sm147, Sm149, Eu151, Gd157, Dy161, Er166, Yb172, Lu175, Hf179, Pb208, Th232, U238, Tb159
Raster			
W	500.9 μm		
H	500.9 μm		
A	2.509 $\times$ 10^5 μm^{-2}		
D	200–400 μm	Sample time	10–60 ms
		Samples per peak	20
		Mass window	60
		Runs	4
		Passes	3
		Total time per sample	01:36

times in Milli-Q H_2O, dried at 100 °C over 60 min and re-weighed to a precision of 0.1 μg established by 200 repeat weighing of a standard. The weight loss of the diamond was used to calculate trace element concentrations. For a typical 180 min ablation of a gem diamond using a 500 $\times$ 500 μm raster, the mass loss was $\sim$600 μg.

4.3.3. ICPMS analysis. Analyses were carried out on a Thermo Scientific Finnigan™ ELEMENT2 double focusing magnetic sector-field ICPMS running at an RF power of 1300 W. Plasma cool gas, auxiliary gas and nebulizer gas flow rates were 16 l min^{-1}, 1 l min^{-1} and $\sim$0.95 l min^{-1} respectively (table 1). The introduction system was initially fitted with a nominal 100 μl min^{-1} micromist glass concentric nebulizer operating at an uptake rate of $\sim$126 μl min^{-1}, together with an ESI quartz dual-pass cyclonic spray chamber. These conditions were used in experiments involving fluid inclusion-rich fibrous and coated diamonds. To improve nebulization efficiency a nominal 50 μl min^{-1} ESI PFA-50 concentric nebulizer was later employed, in conjunction with a dedicated dual-pass spray chamber dedicated to high-purity diamond analyses (table 1).

At the start of the analytical session the mass spectrometer was tuned using an In standard solution. The technique as currently applied collects data on 23 elements (Ti, Rb, Sr, Y, Zr, Nb, Ba, La, Ce, Pr, Nd, Sm, Eu, Gd, Dy, Tb, Er, Yb, Lu, Hf, Pb, Th, U) with a sampling time of 10–60 ms per isotope per scan depending on the abundance of the isotope (table 1). Prior to the analytical session the oxide production rates were checked using 1 ppb solutions of Ba, La, Ce, Pr, Nd, Sm and Gd (Harlou *et al* 2009). Sensitivity is optimized to give low oxide generation whilst maintaining high overall sensitivity and CeO/Ce is maintained at <2%. Elemental and oxide interferences on the mass spectrum of interest were monitored and corrected using the methods outlined in Font *et al* (2007), Harlou *et al* (2009). Instrumental accuracy in the determination of trace element ratios in the ppt concentration range in solution is documented by Harlou *et al* (2009) and for most elemental ratios of interest is between 5 and 10%.

Samples were analyzed against a multi-point (at least 6 points) calibration line derived from several dilutions of standard USGS rock solutions of AGV-1, BHVO-1, and W2. These were diluted 1000 and 5000 times such that the total dissolved solids concentrations were 2 μg ml^{-1} and 0.4 μg ml^{-1} respectively, providing a more appropriate matrix-match for the samples and yielding calibration lines that required less extrapolation into the region of sample analyte concentrations. The accuracy of these calibrations has been documented in detail by Harlou *et al* (2009). Samples were analyzed in batches of five, each sample running for 96 s with a sample rinse check (3% UpA HNO_3 made with UpA H_2O) run in between every sample for 180 s. The USGS rock standards were re-analyzed as 'unknowns' within the sample run to check the consistency of the calibration line. The original calibration blank and separate wash blank are also run at this stage to monitor and later correct potential analytical drift through the session. The limits of quantification for our total procedure are described below.

4.3.4. Analytical blanks, limits of detection and limits of quantification. The high purity of gem-quality diamonds indicated by the early study of Fesq *et al* (1975) and subsequent work by others, in combination with our preliminary studies, demonstrates the need for an analytical technique with very low limits of quantification (LQ), that allow the production of data that are quantitative in nature. When examining this requirement it is important to adhere to a common set of definitions, namely those outlined by Currie (1968, 1999) and adopted by IUPAC, the International Union of Pure and Applied Chemistry. The numerous recent publications reporting methods and data for non-gem, fluid-rich diamonds, do not quote or use the concept of the limit of quantification despite claiming to produce quantitative data (e.g., Rege *et al* 2005, Tomlinson *et al* 2005, Zedgenizov *et al* 2007). Such publications usually record the limit of detection (LOD) for their particular method. The definition of the LOD is: 'the true net signal level that may be expected *a priori* to lead to *detection*' (Currie 1968, p 587). The implication is that while data produced from signals above LOD are detectable they cannot be described as being quantitative unless they exceed the LOQ, defined as: 'the signal level above which a quantitative measurement can be performed with a stated relative uncertainty' (Currie 1968, p 587). While Currie's efforts have brought clarity to the definitions, within the field of analytical geochemistry there is still wide-spread use of the LOD as some sort of validation that quantitative data are being presented when this may not be the case. The LOD defines only the limit of the inherent detection capability in any chemical measurement procedure (Currie 1968, 1999, Olivieri *et al* 2006). Data must exceed LOQ (the minimum quantifiable accurate value) if it to be referred to as truly quantitative (figure 3).

Here we use the expressions derived by Currie (1968, 1999) to derive LOD and LOQ for our new 'off-line' laser sampling method. These expressions are based on hypothesis testing and their graphical expression, together with the underlying assumptions are outlined in figure 3. We employ the expressions for these parameters derived for a situation where the analytical blank is 'well known' and normally distributed. We estimate blank parameters by the 'external approach', i.e., by multiple measurements ($n = 20$) of the total procedural blank analyzed in the period of this study, that encompasses all elements of our chemical and instrumental procedures. For this situation we take our LOQ value to be:

$$\mathrm{LOQ} = 10\sigma_{\mathrm{blank}} \tag{1}$$

and LD is defined as

$$\mathrm{LOD} = 3\sigma_{\mathrm{blank}} \tag{2}$$

where σ_{blank} is the standard deviation of the blank. Following Currie (1999), we attribute errors of 5% to Type I, or 'false positive' decisions and 5% for Type II errors (false negative errors; figure 3) and assign an error for the resulting quantification at 10% or less (Currie 1999). We note that for other methods, such as direct laser ablation ICPMS, where only LOD is usually presented, there is often inadequate information provided to fully evaluate how the 'blank' is defined, making it difficult to judge how adequate the 'blank' will be at capturing the true variability within the system. The lack of detailed provision of this information also causes problems in assessing whether the stated LOD values are likely to be meaningful.

For our measurements, repeatability of blanks yielded consistently low values so that our limits of quantification (LOQ) are <1 pg for most of the analyzed elements, except for Sr, Zr, Ba which range between 2 and 9 pg, and for Pb with an LOQ of ~30 pg (table 2). These levels are consistent with our expectations based on total procedural blank variability for other chemical measurement processes established in our laboratory. Such LOQ values are considerably less than the analyte levels present in most gem diamonds, with the occasional exception of Lu (table 2).

4.3.5. Repeatability. A repeat ablation was made on one diamond plate (1581) to assess the reproducibility of trace element abundances and ratios. There is no *a priori* reason to expect high levels of repeatability in the abundances of trace elements within gem diamonds as it is likely that we are sampling very sparsely distributed fluid inclusions. Repeat measurement of sample 1581 shows that absolute levels of REE and other trace elements are not reproducible to better than 30–50% relative to each other (figures 4 and 5). Of greater importance is the similarity in relative trace element fractionations, both in terms of smooth chondrite-normalized REE patterns with very similar slopes (La_n/Sm_n agree to within 6.3%), and also similar relative depletions in Rb/Ba, negative Sr anomalies and Zr–Hf depletions. Hence, although we are unable to be certain about the repeatability of trace element abundances in gem diamonds, because of likely within-sample heterogeneity due to the heterogeneous distribution of the fluids/melts hosting incompatible elements, we are confident that the data accurately reproduce the relative trace element fractionations displayed by the diamond-forming fluids, even at the very low analyte levels present.

4.3.6. Comparison of analytical methods for trace element analysis in gem diamonds. The very low trace element abundances found in this study confirm the earlier indications of the Fesq *et al* (1975) study, i.e., that gem-quality diamonds contain exceedingly low levels of the incompatible trace elements of interest to geochemists (REE, HFSE, LILE etc). Abundances of almost all incompatible trace elements are in the 10s of ppb to less than 10 ppt range. This presents a considerable analytical challenge for any analytical technique and it is especially severe considering the unusual nature of the diamond matrix that renders it intractable to traditional wet-chemical dissolution techniques that can routinely deal with such low analyte levels (e.g., Font *et al* 2007, Harlou *et al* 2009). The problem for diamond is further accentuated by the lack of an established diamond analytical standard.

The recent application of on-line laser ablation ICPMS to the analysis of fluid-inclusion-rich diamonds, with trace element abundances in the ppm range, has been successful because of the high concentrations of the elements of interest

Table 2. Trace element abundances (wt ppt) determined for the Cullinan, Siberian and Venezuelan diamonds. Quantification is achieved via normalization to the weight loss of the diamond crystals during ablation. Limits of quantification in ppt are provided also, based on a large representative blank set ($n = 20$). (Note: <DL: value below blank value; NR: no value reported/analyzed; NV: no value; Samples: concentration in ppt normalized to the wt loss during ablation; LOQ: values in pg/g.)

	Cullinan	Cullinan	Cullinan	Cullinan	Cullinan	Cullinan	Cullinan	Cullinan	Cullinan	Cullinan	Udac.	Mir	Venezuela	
	Sample # & paragenesis													
	AP25	AP26	AP28	AP30	AP31	AP34	AP35	AP36	AP37	AP38	3812P	1581	5921	LOQ
	E	E	P	P	E	E	E	E	E	E	P	E	?	
Ti	1257 524.4	333 027.4	<DL	<DL	1536 810.6	390 647.8	<DL	<DL	<DL	348 363.4	<DL	551 110.6	22 718.2	2243.0
Rb	13 820.3	2878.1	3058.8	4541.8	6616.6	3377.1	4551.7	5770.6	2853.6	3734.6	16 565.7	13 503.5	<DL	0.2
Sr	16 489.3	17 432.5	4111.4	10 206.7	52 377.1	10 264.9	11 161.4	20 673.6	9294.8	32 383.5	54 859.4	84 698.8	<DL	9.7
Y	1152.4	3474.8	168.2	280.5	4438.0	562.5	2591.7	1705.0	446.8	1456.5	329.0	3595.5	<DL	0.3
Zr	22 389.2	30 555.5	3224.5	16 390.9	39 810.7	20 544.9	30 822.7	4234.3	3965.6	46 444.3	4865.5	49 754.7	72 527.5	5.1
Nb	578.6	4388.5	1310.7	<DL	3203.5	996.8	18 856.7	<DL	608.5	<DL	1734.3	58 637.0	1519.9	0.5
Cs	954.8	378.9	228.5	458.9	687.5	187.0	613.2	432.7	225.1	455.2	NR	16 078.5	21 069.1	14.5
Ba	34 010.7	53 060.7	<DL	29 802.3	57 339.7	13 184.5	69 788.7	34 545.1	5011.1	10 267.5	87 604.1	28 537.2	3728.7	0.5
La	1621.2	3472.2	160.9	617.4	4691.6	15 917.7	3018.5	1544.6	499.1	4161.4	1705.5	52 831.8	7791.0	0.5
Ce	1454.3	4506.5	<DL	1316.5	8735.2	96 302.1	6205.6	1381.3	235.1	19 900.3	2800.2	6348.0	205.1	1.6
Pr	423.8	3317.4	128.2	239.8	3873.3	201.5	3306.2	1018.1	403.8	1906.5	276.3	22 074.7	516.3	0.6
Nd	<DL	1791.7	6881.0	<DL	69 648.7	<DL	7920.0	<DL	<DL	269 979.4	1042.7	3952.4	116.7	2.2
Sm	211.7	2584.9	118.2	168.1	3522.4	62.6	2457.4	595.5	264.2	1871.5	143.7	3311.3	3.0	0.9
Eu	200.6	2672.9	0.8	54.4	2918.9	0.8	2432.1	538.3	155.5	103.6	27.6	864.1	56.5	0.2
Gd	<DL	2660.1	−409.4	<DL	3696.0	<DL	2589.9	582.8	<DL	163.9	<DL	<DL	<DL	0.0
Tb	197.3	2716.4	52.4	161.8	3141.1	55.9	2706.9	761.6	373.0	103.5	12.0	236.5	1.1	0.1
Dy	264.5	2367.6	108.7	157.1	2809.7	166.6	2007.8	701.7	346.2	99.5	63.5	994.6	<DL	0.3
Er	182.8	2394.1	39.0	154.4	2927.0	43.1	2563.9	744.0	268.2	152.9	46.2	264.4	12.0	0.1
Yb	171.1	2631.3	86.4	194.1	3443.8	150.8	2599.8	834.9	401.4	240.8	18.3	208.3	80.1	0.7
Lu	203.1	2675.0	56.4	170.7	3485.0	61.7	2682.6	861.8	396.9	168.5	0.2	26.7	6.6	0.1
Hf	628.0	5090.4	66.9	360.0	3576.7	599.1	20 368.2	563.3	360.5	1874.8	176.2	1511.7	1648.5	0.2
Pb	236 866.7	107 479.3	41 086.1	41 122.8	74 048.5	45 141.3	83 926.6	49 810.5	27 313.4	96 618.8	35 189.8	124 494.8	45 001.9	32.9
Th	436.0	3419.7	137.5	196.6	3200.7	221.5	4694.2	1037.2	496.9	495.4	331.5	5431.8	182.4	0.2
U	178.2	1946.1	92.5	145.1	1508.0	97.8	3118.1	385.7	140.7	246.5	91.0	291.2	31.7	0.0
La/Yb	9.5	1.3	1.9	3.2	1.4	105.5	1.2	1.9	1.2	17.3	93.4	253.6	97.2	
Nb/U	3.2	2.3	14.2	NV	2.1	10.2	6.0	NV	4.3	NV	19.1	201.4	47.9	
Ba/Nb	58.8	12.1	NV	NV	17.9	13.2	3.7	NV	8.2	NV	50.5	0.5	2.5	
Zr/Hf	35.7	6.0	48.2	45.5	11.1	34.3	1.5	7.5	11.0	24.8	27.6	32.9	44.0	

within such diamonds (Resano *et al* 2003, Tomlinson *et al* 2005, 2006, 2009, Rege *et al* 2005, Zedgenizov *et al* 2007, Weiss *et al* 2008a, 2008b). Even in this situation, where abundances are high, the agreement between INAA and on-line LA–ICPMS methods can range between <10% and >400% disparity depending on the element of interest (e.g., Rege *et al* 2005), and this may reflect heterogeneity within fluid-inclusion-rich diamonds. Nonetheless, such studies have produced a wealth of valuable information and advanced our understanding of diamond-forming fluids.

For gem-quality diamonds the situation is quite different because of the extremely low analyte levels involved and this is reflected by the lack of published trace element data via on-line LA–ICPMS for gem diamonds. The analyte concentration levels reported by us in table 2 for gem-quality diamonds are below the stated detection limits for published on-line LA–ICPMS methods for many incompatible trace elements and are almost certainly below any realistic estimate of the limits of quantification for that method, when detection limit data are scaled up to the 10-sigma level.

The problem of the very low trace element abundances present in gem diamonds can be understood clearly when the total number of ions available to be counted by the mass spectrometer detection system is calculated for a typical direct laser ablation pit. To illustrate the problem, consider a hypothetical direct ablation LA–ICPMS analysis of Udachnaya sample 3812 (table 2). This sample contains 1.7 ppb La, 0.144 ppb Sm and 0.018 ppb Yb. If we produce a typical 100 μm diameter by 100 μm deep cylindrical laser pit and apply the analytical parameters stated by Rege *et al* (2005), i.e., 130 s analysis time with 40 isotopes measured and a dwell time of 30 ms, we should detect approximately 3000 total ions of La, ∼240 total ions of Sm and only 27 total ions of Yb, assuming a conservative ion-transfer efficiency (sample to detector) of 0.1%. This limits the maximum theoretical precision achievable, from counting statistics alone, of between 28 and 40% for Yb. When considered as a likely signal size at the ion detector, this total yield of 3000 ions will result in between 30 and 60 counts per isotope sampling (30 ms dwell time) in any given mass scan for La; between 2 and 5 counts for Sm and as little as 0.25–0.5 ions for Yb depending on the assumed ion transmission efficiencies. These efficiencies can vary between 0.03 and 0.1% for laser ablation and solution sampling, with solution sampling usually being more efficient (Nowell and Horstwood 2009). Even when these values are converted to 'counts per second' it is obvious that the on-peak background signal stability for direct ablation will need to be better than: 190 cps (La), 15 cps (Sm) and 1.7 cps (Yb) in order for quantitative data to be obtained. From these considerations, of the three REE selected, only La is likely to be at or above the limits of quantification for most direct on-line ablation methods. For more abundant elements such as Sr (∼50 ppb in 3812), the problem is much less severe and it is likely that quantitative data could be produced. In contrast, the larger sampling volume (and mass) resulting from the significantly larger ablation raster grid created during our closed-system ablation procedure results in almost 30 times more analyte signal, assuming similar ion transport efficiency between laser- and solution introduction systems. This yield will obviously be greater still if we achieve the normally more efficient ion transfer (solution to detector) achieved by solution-based ICPMS methods. This greater improvement will be off-set slightly by any losses in transferring the ablated material from our closed cell to the analyte solution. When these gains in total analyte signal are considered for the closed-system ablation method described above, we require background stabilities better than 4600 cps (La), 358 cps (Sm) and 40 cps (Yb), at the 10-sigma level, for quantitative data. This is easily achieved for La and Sm and most instrument sessions attain this performance for Yb. Hence, from consideration of ion yields alone, the increased total analyte budgets that result from the larger sampling mass of the closed-system ablation method we describe here are more likely to produce quantitative analytical data on gem-quality diamonds compared with direct ablation techniques.

An additional advantage with the off-line ablation technique that uses solution analysis as a sample introduction method, is that we can use robust signal calibration procedures based on well documented international standards in solution. Calibration lines are multi-point and uncertainties in calibration can be easily and quantitatively propagated into the final uncertainties on measurements. Hence we do not require a homogeneous, matrix-matched standard of the sort usually required for direct 'on-line' laser ablation studies. This is a considerable benefit in the absence of any recognized diamond analytical standard.

Drawbacks to our method are obvious. We typically ablate a larger pit size than direct on-line ablation methods but consider the improvements in analyte yield outweigh this factor. We note that the production of any surface pit generated by laser-produced beams on a diamond surface leads to that diamond being regarded in trade-terms as 'treated'. Hence the fractionally larger pit produced by our method will not lead to grossly different devaluation of any given diamond. A clear consequence of our analytical procedure is the greater time taken to analyze samples compared with direct on-line laser ablation approaches. Clearly, this is a specialized technique designed for low sample throughput, and highest data quality. However, from the small database for gem diamonds reported in table 2 and consideration of likely limits of quantification, we suggest that the higher throughput direct ablation methods are not yet capable of producing quantitative data (as defined by exceeding a rigorously derived method limit of quantification) for a wide range of trace elements in gem diamonds. We provide a method that solves this problem.

5. Results

5.1. CL characteristics/FTIR results

The 10 Cullinan samples exhibit octahedral zonation, with the intensity of blue luminescence correlating with nitrogen content. Dark areas of luminescence are commonly associated with mineral inclusions, particularly eclogitic garnets.

The lherzolitic Type II diamond AP30 is an irregular resorbed aggregate and exhibits very unusual CL patterns

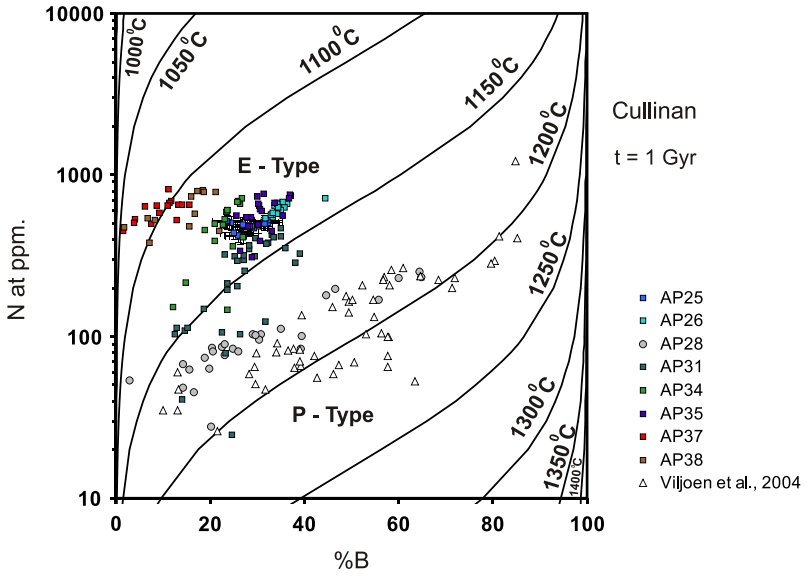

Figure 2. Total N (atomic ppm) versus nitrogen aggregation expressed as per cent as B defects for some of the Cullinan diamonds analyzed in this study. The eclogitic and peridotic areas are spatially separated and a low and high aggregation states can be observed. Also plotted are data on diamonds from a single peridotite xenolith from Cullinan mine studied by Viljoen *et al* 2004.

within nested octahedral growth zones. This diamond shows similar high levels of resorption to AP28, also a P-type diamond. Hence, both P-type diamonds appear more highly resorbed than the E-type diamonds. All resorbed peridotitic stones show evidence of plastic deformation in their CL images whereas a single un-resorbed, undeformed P-type diamond within this suite led Chinn *et al* (2003) to suggest two populations of P-type diamonds at Cullinan.

The Type I Cullinan diamonds can be divided into groups with high and low nitrogen aggregation (Chinn *et al* 2003; figure 2). The highly aggregated Type I samples have greater than 40% B-aggregated nitrogen. Trends of total nitrogen content versus nitrogen aggregation state, expressed as %B-center, show that although there is variation within individual diamonds, the internal zonation trends approximate to theoretical isothermal trends previously established to be characteristic for Cullinan diamonds (Viljoen *et al* 2004; figure 2).

P-type sample AP28 has low N (<200 ppm) and very variable levels of N-aggregation across the traverse. The changes in total nitrogen content within AP28 are generally mirrored by the nitrogen aggregation state and platelet peak area, suggesting single-stage growth at constant temperature. The slope of the trend indicates that this diamond resided at an integrated mantle residence temperature that was significantly above that of the other Cullinan diamonds. Sample AP28 is P-type and shows similar low N at highly variable %B to >30 individual diamonds recovered from a peridotite xenolith from Cullinan (Viljoen *et al* 2004) and hence may belong to that diamond population.

A detailed study of the growth features of Siberian diamonds as revealed in CL has been published by Bulanova (1995) and samples 3812 and 1581 originate from the same sample suite. Both samples show simple octahedral growth patterns throughout.

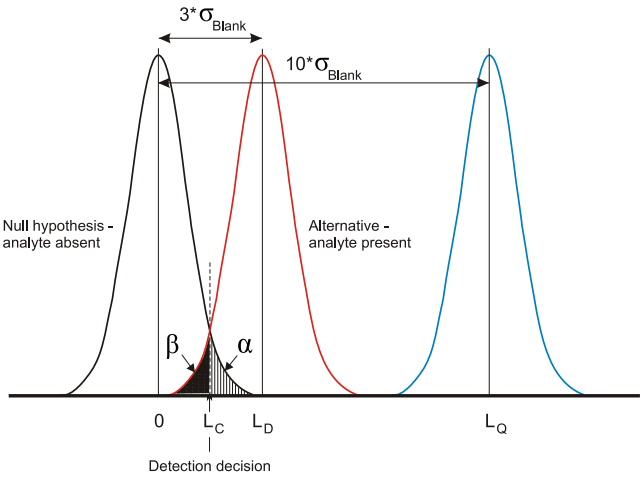

Figure 3. Illustration of the definitions of LD and LQ used in the text. For presentation of the defining relations, L is used as the generic symbol for the quantity of interest. Subscripts C, D, and Q are used to denote the critical value, detection limit, and quantification limit, respectively. The maximum acceptable false positive together with the standard deviation of the net signal of the null establish the critical value, L_C (detection decision), upon which decisions may be based. An observed signal must exceed L_C to be detected. Once L_C has been defined, the detection limit L_D may be established by specifying L_C, the acceptable level, β and the standard deviation σ_D which characterizes the probability distribution of the net blank signal when its true value is equal to L_D.

5.2. Trace element characteristics

Chondrite-normalized trace element patterns of the Cullinan diamond suite and other gem diamonds from Siberia and Venezuela are very low, ranging from 10s of ppb to 10s of ppt by weight, with only Ti exceeding 1 ppm. All samples are highly depleted relative to chondritic abundances but elemental concentrations vary widely (between 0.1 and

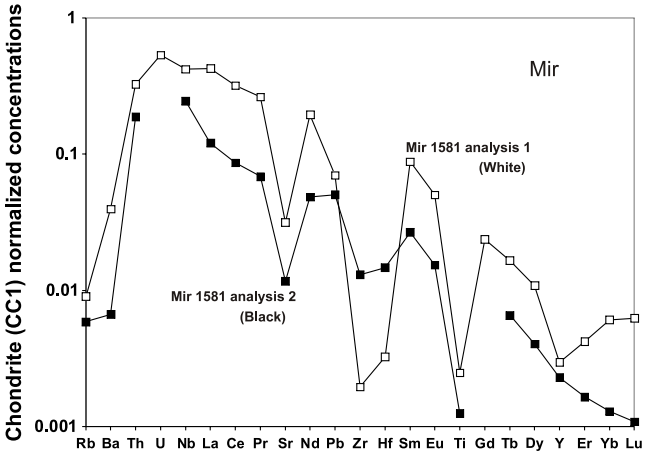

Figure 4. Full-method replicate analysis on the Mir 1581 fluid-microinclusion-poor diamond showing similar overall patterns and deviations of <50% (relative) in concentrations.

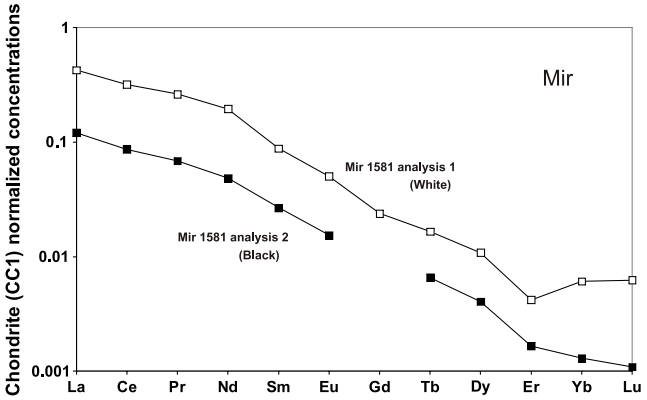

Figure 5. Full-method replicate analysis on the Mir 1581 fluid-microinclusion-poor diamond focusing on the smooth REE patterns.

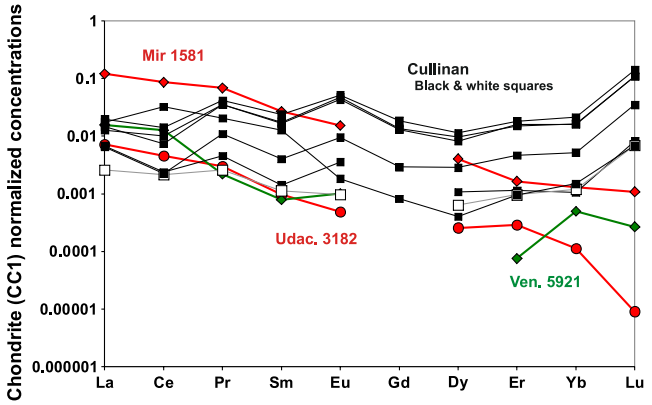

Figure 6. Chondrite-normalized trace elemental concentrations in the Cullinan, Siberia and Venezuela diamonds analyzed in this study.

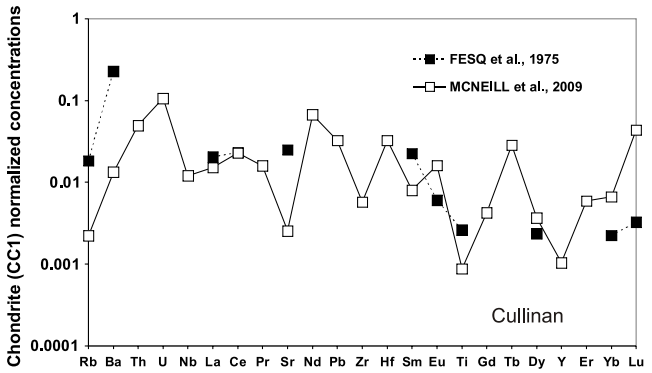

Figure 7. Average trace element abundances determined here for Cullinan gem diamonds plotted with the average values for a more restricted range of elements from Cullinan diamonds presented by Fesq *et al* (1975) based on INAA.

0.0001 × chondrite). HREE along with Y, Nb, Cs range from 0.1 to 1 ppb. Some odd atomic number REE such as Eu can be present at concentrations of less than 10 ppt. Large ion lithophile elements (LILE) such as Rb and Ba, vary from 2 to 30 ppb while U values are between 0.1 and 1 ppb (table 2). Pb reaches several ppb and forms a positive anomaly in all normalized trace element patterns. Ti ranges from ppb values up to 2 ppm.

All chondrite-normalized trace element patterns show enrichment of light rare earth elements (LREE) compared to heavy rare earth elements (HREE), with La_n/Yb_n ratios of 1.3–105.5. In all of the gem-quality diamonds we have analyzed, trace element abundances broadly decrease with increasing elemental compatibility into a solid (figures 1 and 6). As a suite, the Cullinan diamonds analyzed here are characterized by negative Nb, Sr, Zr, Ti and Y anomalies and positive U, Nb, and Pb anomalies (figure 1). All samples in our suite have negative Sr anomalies except the Udachnaya P-type diamond, 3812. Average trace element abundances determined here for Cullinan gem diamonds generally compare well with the average values for a more restricted range of elements from Cullinan diamonds presented by Fesq *et al* (1975) except that Sr is more elevated in the Fesq *et al* data (figure 7).

Although of much lower absolute abundances, the Cullinan gem-diamond inter-element fractionations are broadly similar to those observed in Botswana and Congo fluid-rich diamonds (Klein-BenDavid *et al* 2008) and some fluid-rich diamonds from Kankan (Weiss *et al* 2008a, 2008b), that show LILE enrichment and prominent depletions in Zr, Hf and Sr (figure 1).

While the two Siberian gem-quality diamonds show the same low levels of REE and general level of LREE/HREE enrichment as the Cullinan diamonds (La_n/Yb_n = 93.4–253.6; figure 1), only the Mir diamond, 1581, shows the pronounced LILE enrichment seen in some of the Cullinan diamonds. The P-type sample from Udachnaya (3812) shows a much flatter multi-element normalized pattern than the Cullinan samples, similar to the normalized patterns for fluid-rich diamonds from the same kimberlite pipe (Udachnaya) reported by Zedgenizov *et al* 2007; figure 8). The Venezuela diamond PHN5921 shows similar trace element characteristics to 3812, with no pronounced enrichment of LILE over Nb.

In the current small data set for gem-quality diamonds we can see no consistent differences between the E- and P-type parageneses.

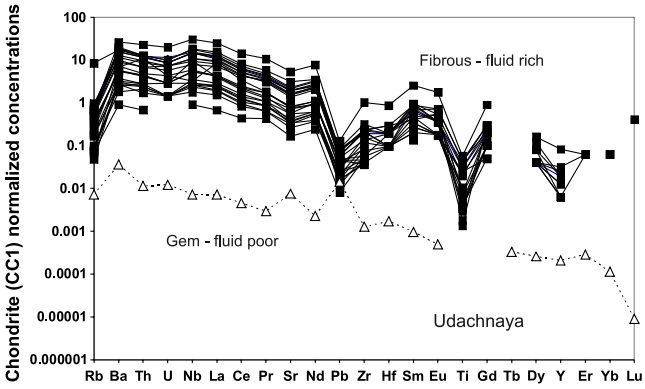

Figure 8. Comparison between trace element patterns determined here for a gem diamond from Udachnaya and those produced by Zedgenizov *et al* 2007 from fibrous diamonds in the sample kimberlite.

6. Discussion

6.1. CL, FTIR

Nitrogen data from infra-red traverses confirm the low nitrogen (or Type II) nature of at least one of the Cullinan diamonds (AP30). Other diamonds show dark zones in CL, often close to garnet inclusions. Chinn *et al* (2003) suggest that aluminum (an electron acceptor) from the garnet may act as a 'getter' for the nitrogen, which is an electron donor, to produce low-N (type II) diamond around garnet inclusions. However, the origin of these features remains uncertain. Secondary Ion Mass Spectrometry (SIMS) analysis would be required to demonstrate whether the nitrogen contents of these areas are significantly lower than areas of bright luminescence, or whether the nitrogen is contained in infra-red inactive defects together with carbon (as opposed to nitrogen).

AP30 (Type II) exhibits weak dark blue luminescence. Because the diamond is nitrogen free, the observed zonation is not due to different levels of infra-red active nitrogen impurities, but may be related to differences in plastic deformation levels. Deformation-induced lamination lines were observed on the stone prior to polishing.

The highly varied N-aggregation characteristics of the relatively small number of Cullinan diamonds analyzed here combined with that observed in other studies of a Cullinan diamondiferous peridotite xenolith (Viljoen *et al* 2004) indicate significant variation in mantle residence histories (age or thermal histories) present in the diamonds sampled by the Cullinan kimberlite. Within just the suite analyzed here, the distinct N-aggregation characteristics of the low- and high aggregation groups of Type I diamonds indicates at least two separate populations of diamonds that have experienced differing lithospheric residence conditions (Chinn *et al* 2003). In addition, the very distinct N-aggregation characteristics of sample AP28 indicate that it has experienced a history distinct from the two main populations identified above. The within-diamond zonation trend of N content and aggregation state of sample AP28 falls on the same isothermal trend as the multiple diamonds from a single xenolith studied by Viljoen *et al* (2004) and is much more regular than the 'run-of-mine' production from Cullinan (Chinn *et al* 2003). The N-aggregation systematics of AP28 and the diamonds studied by Viljoen *et al* (2004) appear distinct from the main 'high aggregation' suite at Premier and may suggest an additional population of diamonds at this mine (Chinn *et al* 2003). Hence there may be at least three different generations of diamonds present at Cullinan. Such age variation has been suggested on the based of diamond inclusion dating studies (Richardson *et al* 1993) but we cannot relate the diamonds examined in that study to our own because of the lack of available N-aggregation data.

6.2. Elemental geochemistry

The multi-element, chondrite-normalized trace element patterns of the Cullinan gem diamonds have several characteristics in common with fluid-inclusion-rich fibrous diamonds from locations such as Botswana and the Congo (Klein-BenDavid *et al* 2008), Kankan (Weiss *et al* 2008a, 2008b) and Ekati, N. Canada (Tomlinson *et al* 2006). The most obvious similarity is the high normalized LILE abundances relative to Nb and pronounced negative Sr anomalies. However, the Cullinan gem diamonds do not have the pronounced negative HFSE (Hf, Zr, Ti) anomalies relative to REE seen in the fluid-inclusion-rich diamonds.

The gem diamond from the Mir kimberlite (Siberia) also shows LILE enrichment akin to the Cullinan stones and may have formed from similar diamond-forming fluids. In contrast, the gem diamond from Udachnaya (3812) has much less pronounced LILE enrichment than those from Cullinan and, although abundances differ, the general trace element fractionation signature is similar to that seen in fluid-rich fibrous diamonds from the same kimberlite (Zedgenizov *et al* 2007). Although the data are more noisy, the P-type diamond from Venezuela (PHN 5921) is similar to the Udachnaya diamond in terms of its trace element systematics.

While our sample numbers are small so far, we can begin to make some general comparisons between the fluids responsible for forming fluid-rich, fibrous diamonds and those forming octahedral, gem-quality diamonds. The trace element systematics seen in the gem diamonds appear, broadly, to be similar to those seen in fluid-rich diamonds from a variety of locations. From the trace element variability observed in fluid-rich diamonds, Weiss *et al* (2008a, 2008b) have suggested the existence of two end members of diamond-forming fluids that follow the broad sub-divisions observed here, with the key criteria being the levels of enrichment in LILE relative to Nb. Our small database for gem-quality diamonds indicates that many of the same differences in elemental systematics exist in the parental fluids to these diamonds.

Calculations of the trace element signature of fluids in equilibrium with silicate inclusions within gem and fibrous diamonds, in comparison with the measured trace element systematics from fluid-inclusion-rich diamonds, have provided evidence that the fluids involved in the growth of both gem diamonds and fluid-rich fibrous diamonds could share the same origin (Tomlinson *et al* 2009). Our observed similarities for

the fluid signature of the diamonds provides further support for this suggestion. At present, the database for quantitative trace element characteristics in fluid-poor, gem diamonds is too small to warrant further speculation on the origins of gem diamonds and progress will involve detailed trace element studies of diamonds that have been well characterized in terms of solid mineral inclusions (e.g., Stachel and Harris 2008) and where C and even N isotope measurements have been made to help constrain the overall nature and range in fluid types that these diamonds may crystallize from (e.g., Stachel *et al* 2009).

7. Conclusion

We present a method for the quantitative analysis, at low ppt levels, of trace elements within fluid-poor gem diamonds that uses laser ablation in a closed cell to access impurities containing trace elements and then pre-concentrates the analytes into solution for determination by sector-field ICPMS using multi-point calibration lines. We evaluate the instrumental/method parameters necessary for the production of truly quantitative data, and show that the large ablation pit sizes employed in our closed-system ablation approach are likely to lead to considerably enhanced limits of quantitation. In order to effectively compare data there is a need for all researchers involved in diamond trace element analysis to provide well documented estimates of their limits of quantitation.

Examination of a suite of 10 diamonds from the Cullinan Mine, South Africa, along with other diamonds from Siberia (Mir and Udachnaya) and Venezuela confirms that the concentrations of incompatible trace elements are very low and highly depleted relative to chondritic abundances. HREE along with Y, Nb, Cs range from 0.1 to 1 ppb. Some REE such as Eu can be present at concentrations of less than 10 ppt. Large ion lithophile elements (LILE) such as Rb, Ba, vary from 2 to 30 ppb while U values are extremely low, between 0.1 and 1 ppb. Ti ranges from ppb values up to 2 ppm.

Examination of chondrite-normalized multi-element data reveals the presence of two general kinds of diamond-forming fluids within the gem diamonds. One group displays enrichments in large ion lithophile elements (LILE: Ba, U, La) over Nb. The other has normalized LILE abundances more similar to Nb and has less fractionated chondrite-normalized trace element patterns in general. These two groups bear some similarity to different groups of fluids observed in fluid-inclusion-rich diamonds (Weiss *et al* 2008a, 2008b), providing some supporting evidence for a link between the parental fluids for both fluid-rich and gem diamonds suggested from silicate inclusion chemistry (Tomlinson *et al* 2009).

Acknowledgments

This work was done during the tenure of a Diamond Trading Company/De Beers student scholarship for JM and a Marie Curie fellowship at Durham for OKBD. We thank De Beers, Peter Nixon and the Institute for Diamonds, Yakutsk, for samples and Thomas Stachel for a constructive review of the manuscript.

References

Akagi T and Matsuda A 1998 Isotopic and elemental evidence for a relationship between kimberlite and Zaire cubic diamonds *Nature* **366** 665–7

Bibby D M 1982 Impurities in natural diamond *Phys. Chem. Carbon* **18** 3–91

Boyd S R, Kiflawi I and Woods G S 1994 The relationship between infrared absorption and the A defect concentration in diamond *Phil. Mag.* B **69** 1149–53

Boyd S R, Kiflawi I and Woods G S 1995 Infrared absorption by the B Nitrogen aggregate in diamond *Phil. Mag.* B **71** 351–61

Bulanova G P 1995 The formation of diamond *J. Geochem. Explor.* **53** 1–23

Chinn I, Pienaar C and Kelly C 2003 Diamond growth histories at Premier Mine *8th Int. Kimberlite Conf., Extended Abstracts*

Currie L A 1968 Limits for qualitative detection and quantitative determination *Anal. Chem.* **40** 586

Currie L A 1999 Detection and quantification limits: origins and historical overview *Anal. Chim. Acta* **391** 127–34

de Wit M J, de Ronde C E J, Tredoux M, Roering C, Hart R J, Armstrong R A, Green R W E, Peberdy E and Hart R A 1992 Formation of an Archaean continent *Nature* **357** 553–62

Deines P, Gurney J J and Harris J W 1984 Associated chemical and carbon isotopic composition variations in diamonds from Finsch and Premier kimberlite, South Africa *Geochim. Cosmochim. Acta* **48** 325–42

Fesq H W, Bibby D M, Erasmus C S, Kable E J D and Sellschop J P F 1975 Determination of trace element impurities in natural diamonds by instrumental neutron activation analysis *Physics and Chemistry of the Earth* vol 9, ed L H Aherns, J B Dawson, A R Duncan and A J Erlank (Oxford: Pergamon) pp 817–36

Font L, Nowell G M, Pearson D G, Ottley C J and Willis S G 2007 Sr isotope analyses of bird feathers by TIMS: a tool to trace bird migration and breeding *J. Anal. At. Spectrom.* **22** 513–22

Harlou R, Pearson D G, Nowell G M, Ottley C J and Davidson J P 2009 Combined Sr isotope and trace element analysis of melt inclusions at sub-ng levels using micro-milling, TIMS and ICPMS *Chem. Geol.* **260** 254–68

Izraeli E S, Harris J W and Navon O 2004 Fluid and mineral inclusions in cloudy diamonds from Koffiefontein, South Africa *Geochim. Cosmochim. Acta* **68** 2561–75

Kinny P D, Griffin B J, Heaman L M, Brakhfogel F F and Spetius Z V 1997 Shrimp U–Pb ages of perovskite from Yakutian kimberlites *Russ. Geol. Geophys.* **38** 97–105

Klein-BenDavid O, Pearson D G, Cantigny P and Nowell G M 2008 Origins of diamond forming fluids—constraints from a coupled Sr–Nd isotope and trace element approach *9th Int. Kimberlite Conf., Extended Abstracts* 9IKC-A-00118

Maas R, Kamenetsky M B, Sobolev A V, Kamenetsky V S and Sobolev N V 2005 Sr, Nd, and Pb isotope evidence for a mantle origin of alkali chlorides and carbonates in the Udachnaya kimberlite, Siberia *Geology* **33** 549–52

Navon O, Hutcheon I D, Rossman G R and Wasserburgh G J 1988 Mantle derived fluids in diamond micro-inclusions *Nature* **335** 784–9

Nixon P H, Griffin W L, Davies G R and Condliffe E 1994 Cr garnet indicators in Venezuela kimberlites and their bearing on the evolution of the Guyana craton *Proc. 5th Int. kimberlite Conf.* ed H O A Meyer and O Leonardos, pp 378–87, CPRM Speical Publication, 1/A, Brasilia

Nowell G M and Horstwood M S A 2009 Comments on Richards *et al* Journal of Archaeological Science 35, 2008 'Strontium isotope evidence of Neanderthal mobility at the site of Lakonis, Greece using laser-ablation PIMMS' *J. Archaeol. Sci.* **36** 1334–41

Olivieri A C, Faber N M, Ferré J, Boqué R, Kalivas J H and Mark H 2006 Uncertainty estimation and figures of merit for multivariate calibration *Pure Appl. Chem.* **78** 633–61

Pearson D G, Kelley S P, Pokhilenko N P and Boyd F R 1997 Laser $^{40}Ar/^{39}Ar$ dating of phlogopites from southern African and Siberian kimberlites and their xenoliths: constraints on eruption ages, melt degassing and mantle volatile compositions *Russ. Geol. Geophys.* **38** 106–17

Pearson D G, Shirey S B, Bulanova G P, Carlson R W and Milledge H J 1999 Single crystal Re–Os isotope study of sulfide inclusions from a zoned Siberian diamond *Geochim. Cosmochim. Acta* **63** 703–12

Rege S, Jackson S, Griffin W L, Davies R M, Pearson N J and Orielly S Y 2005 Quantitative trace-element analysis of diamond by laser ablation inductively coupled plasma mass spectrometry *J. Anal. At. Spectrom.* **20** 601–11

Resano M, Vanhaecke F, Hutsebaut D, de Corte D and Moens L 2003 Possibilities of laser ablation-inductively coupled plasma-mass spectrometry for diamond fingerprinting *J. Anal. At. Spectrom.* **18** 1238–42

Richardson S H, Harris J W and Gurney J J 1993 Three generations of diamonds from old continental mantle *Nature* **366** 256–8

Schrauder M, Koeberl C and Navon O 1996 Trace element analysis of fluid bearing diamonds from Jwaneng, Botswana *Geochim. Cosmochim. Acta* **60** 4711–24

Schrauder M and Navon O 1994 Hydrous and carbonatitic mantle fluids in fibrous diamonds from Jwaneng, Botswana *Geochim. Cosmochim. Acta* **58** 761–71

Spetsius Z V and Taylor L A 2008 *Diamonds of Siberia. Photographic Evidence for their Origin* (Tennessee: Tranquility Base Press) p 278

Stachel T and Harris J W 2008 The origin of cratonic diamonds—constraints from mineral inclusions *Ore Geol. Rev.* **34** 5–32

Stachel T and Harris J W 2009 Formation of diamond in the Earth's mantle *J. Phys.: Condens. Matter* **21** 364206

Tomlinson E, de Schrijver I, de Corte K, Jones A P, Moens L and Vanhaecke F 2005 Trace element compositions of submicroscopic inclusions in coated diamond: a tool for understanding diamond petrogenesis *Geochim. Cosmochim. Acta* **69** 4719–32

Tomlinson E L, Jones A P and Harris J W 2006 Co-existing fluid and silicate inclusions in mantle diamond *Earth Planet. Sci. Lett.* **250** 581–95

Tomlinson E L, Müller W and EIMF 2009 A snapshot of mantle metasomatism: trace element analysis of coexisting fluid (LA-ICP-MS) and silicate (SIMS) inclusions in fibrous diamonds *Earth Planet. Sci. Lett.* **279** 362–72

Viljoen K S, Dobbe R, Smit B, Thomassot E and Cartigny P 2004 Petrology and geochemistry of a diamondiferous lherzolite from the Premier diamond mine, South Africa *Lithos* **77** 539–52

Weiss Y, Griffin W L, Elhlou S and Navon O 2008b Comparison between LAM-ICPMS and EMPA analysis *Chem. Geol.* **252** 158–68

Weiss Y, Griffin W L, Harris J W and Navon O 2008a Diamond-forming fluids and kimberlites: the trace element perspective *9th Int. Kimberlite Conf. Extended Abstract No. 9IKC-A-00113*

Zedgenizov D A, Rege S, Griffin W L, Kagi H and Shatsky V S 2007 Composition oftrapped fluids in cuboid fibrous diamonds from the Udachnaya kimberlite: LAMICPMS analysis *Chem. Geol.* **240** 151–62